COBEM 2021 26th International Congress of Mechanical Engineering
ABCM Associação Brasileira de Engenharia e Ciências Mecânicas
November 22-26, 2021, Virtual Congress, Brazil

COB-2021-0167
A NUMERICAL STUDY ON THE EFFECTS OF MESH REFINEMENT, ARTIFICIAL DISSIPATION, AND FREESTREAM TURBULENCE ON LAMINAR-TURBULENT TRANSITION PREDICTIONS

Aline Roberta Santos Righi
Leonardo Motta Maia de Oliveira Carvalho
Instituto Tecnológico de Aeronáutica, 12228-903 São José dos Campos, Brazil
alinerighi29@gmail.com, leonardo.mmoliva@gmail.com

Gustavo Luiz Olichevis Halila
João Luiz F. Azevedo
Instituto de Aeronáutica e Espaço, 12228-904 São José dos Campos, Brazil
gustavohalila@gmail.com, joaoluiz.azevedo@gmail.com

Abstract. *The aerospace industry has been using CFD methods as an integral part of its design and development processes for quite some time and, as expected, the methods and the protocols for their use have matured considerably. There are, however, a few areas within aerospace applications for which some challenges for the more widespread use of CFD remain. One of such challenging areas concerns the appropriate treatment of laminar-turbulent transition in high Reynolds number flows over general configurations. The present work is concerned with the study of the impact of mesh refinement and numerical parameters on the accuracy of transition predictions for high Reynolds number flows. The approach adopted here uses a Reynolds-averaged Navier-Stokes formulation, with the SST model for turbulence closure. The SST model is further coupled to the Langtry–Menter transition model. Our investigation goals include the understating of the mesh influence over solutions for bypass and Tollmien-Schlichting (TS) transition mechanisms when using the the Langtry-Menter model and the influence of the freestream viscosity ratio over the numerical solutions for both transition mechanisms. The Langtry-Menter model is implemented in an in-house code named BRU3D. Test cases include a flat plate geometry and the NLF(1)-0416 airfoil. For the TS-wave transition mechanism, the main conclusion is that increasing the freestream eddy viscosity ratio and decreasing the artificial dissipation lead to an upstream movement of the transition front, while the opposite behavior is observed for the bypass mechanism. Similar conclusions are drawn for the NLF(1)-0416 airfoil test case with TS-triggered transition, except that there is no sensitivity in the results related to the effects of artificial dissipation.*

Keywords: *CFD, Laminar-Turbulent Transition, Langtry-Menter Model, Mesh Size.*

1. INTRODUCTION

For many decades, computational fluid dynamics (CFD) techniques have been used in different academic applications or for industrial purposes. Such techniques have been continuously enhanced to allow numerical solutions of increasingly complex fluid flow phenomena. Numerical simulations are applied in research, development, and manufacturing of vehicles in the aerospace industry (Versteeg and Malalasekera, 2007), as well as for academic purposes. However, there are still a few areas within aerospace applications for which some challenges for the more widespread use of CFD remain.

One of such challenging areas is the correct treatment of the laminar-turbulent transition. In the typical path to turbulence, a laminar boundary layer base flow is excited by external forcing such as roughness, sound, vibration, and freestream turbulence through a mechanism referred to as receptivity. Depending on the spectral content of these excitations and on the base flow itself, the hydrodynamic modes can be amplified, leading to bifurcation to turbulence. In the transition region, it is common to use an intermittency function, which is the probability of a given flow region to be turbulent, to model the transition process. Transition to turbulence can be triggered through different mechanisms. In aerospace applications, Tollmien-Schlichting waves (Klebanoff *et al.*, 1962), bypass transition (Ghasemi *et al.*, 2014), and crossflow vortices (Saric and Dagenhart, 1999) are the most common mechanisms causing turbulence. The transition phenomena have an important role in several engineering applications. In high-lift devices, where each element may present Reynolds numbers sufficiently small to sustain laminar flow, the inclusion of transition effects in the numerical simulations improves the agreement with experimental data (Halila *et al.*, 2019a). Additionally, aircraft configurations not originally designed to preserve laminar flow may present transitional regions (Halila *et al.*, 2016, 2018), which further

indicates the relevance of investigating the physics of transition to turbulence. The inclusion of transition effects in CFD codes also makes possible the aerodynamic shape optimization (ASO) of natural laminar flow configurations (Halila *et al.*, 2020; Shi *et al.*, 2020).

Distinct modeling strategies are available to investigate transition to turbulence. Wall-resolved large eddy simulations (LES) and direct numerical simulations (DNS) can be used to investigate transitional flows, but their computational costs are still prohibitive when complex, high-Reynolds number airplane configurations are considered. Flow stability analysis can be used to track the stability modes evolution in temporal or spatial frameworks. Growth rates can then be computed based on the stability modes amplitudes, which are solutions to the stability problem. Boundary-layer effects can be included (Halila *et al.*, 2021). The transition onset point is usually predicted using linear stability methods with the aid of the e^N method (Smith and Gamberoni, 1956), which uses information of the growth rates to compute the N-envelope. Once the transition location is computed, an intermittency function can be used to modify the originally fully-turbulent Reynlods-Averaged Navier–Stokes (RANS) model (Halila *et al.*, 2019b). The most relevant shortcomings related to the industrial use of flow stability approaches are the difficulty in combining these methods with parallelization techniques and the complexity associated with the framework, which usually involves, at least, a boundary layer code, a flow stability code, and the CFD application itself.

In order to address the issues associated with the use of flow stability analysis methods, modified RANS models that are able to predict transition to turbulence were proposed. These models usually augment a standard, fully-turbulent RANS model with one or two additional transport equations. These equations are based on empirical correlations and should ideally be based on local parameters only, so that wall-normal integrations are not required. The Langtry-Menter (LM) transition model (Langtry and Menter, 2009) (LCTM - Local Correlation-based Transitional Model) was developed with the goal of only using local variables. In order to achieve locality, the LM model correlates the momentum thickness Reynolds number, Re_θ, to the strain-rate Reynolds number, Re_ν, which is a local variable (Langtry and Menter, 2009). Many extensions of the Langtry-Menter model have been developed throughout the years and published in the literature.

Important aspects of the correct treatment of transition to turbulence in CFD codes are the capability of correctly predicting the transition onset point for a particular mechanism of transition, the transition region modeling, and the turbulent region computation. These aspects directly impact the aerodynamic coefficients estimation. In this paper, we investigate the impact of mesh refinement and freestream turbulence boundary conditions on the LM model capability to correct represent transitional flows over flat plate and airfoil test cases. For the former, we consider both bypass and TS-triggered transition, while the airfoil test case corresponds to transition caused by the amplification of TS waves.

The rest of this paper is organized as follows. In Sect. 2. the overall formulation of the CFD tool and the Langtry-Menter model are introduced. Numerical results for flat plate test cases are presented in Sect. 3. while airfoil simulations are presented in Sect. 4. The paper is concluded with some closing remarks in Sect. 5.

2. THEORICAL AND NUMERICAL FORMULATION

This section introduces the overall formulation of the CFD tool used for the development of the present paper. Moreover, it also introduces the Langtry-Menter transition model, which is the base model for all tests cases and investigations presented in the next section.

2.1 Overall Formulation of the CFD Tool

In the present work, the Langtry-Menter transition model is implemented in an in-house developed CFD code, BRU3D (Bigarella, 2007; Carvalho *et al.*, 2018), which has been continuously improved by the research group over the years. The code can solve the compressible Euler equations and/or the Reynolds-averaged Navier-Stokes equations. Turbulence closure can be achieved with several different turbulence models, including, for instance, the Spalart-Allmaras model (Spalart and Allmaras, 1994) and the Shear Stress Transport (SST) model (Menter, 1994), among many others. Results that demonstrate the validation of the code with these different turbulence models can be found in Bigarella and Azevedo (2007). Moreover, more recently, the laminar-turbulent transition LM model (Langtry and Menter, 2009) has also been implemented in the code. The equations are solved in a standard, cell-centered, finite volume method for general unstructured grids. Furthermore, the code can be executed in parallel using MPI calls.

In the present case, more specifically, the LM transition model (Langtry and Menter, 2009) is coupled to the SST turbulence model (Menter, 1994). The SST closure combines characteristics of two turbulent closures, namely, the $\kappa - \omega$ model (Wilcox, 1994, 2008) is used in the inner part of the boundary layer and the $\kappa - \epsilon$ (Chien, 1982) is activated in the outer part of the boundary layer. A blending function, as indicated in Eq. (1), is used to switch between both formulations of the model,

$$F_1 = \tanh(\Gamma^4) \tag{1}$$

where $\Gamma = \min\left[\max\left(\Gamma_1, \Gamma_2\right), \Gamma_3\right]$ and Γ_1, Γ_2, and Γ_3 are terms associated to the length scales based on the turbulent length scale, the viscous length scale, and on the cross-diffusion term (Menter, 1994). The SST closure was used as the

base model upon which the Langtry-Menter $\gamma - Re_\theta$ transition model was constructed in the original references to this later model. More information and the complete formulation of the SST model can be found in Menter (1994).

2.2 Langtry-Menter Transition Model

The Langtry-Menter $\gamma - Re_\theta$ (Langtry and Menter, 2009) correlation-based transition model is composed of two transport equations to represent the transition phenomena, in addition to the equations for the SST (Menter, 1994) turbulence model. As mentioned before, the LM model is based on only local variables in order to be compatible with modern CFD codes. Some physical parameters that are relevant in transition prediction cannot be computed locally because wall-normal integrations are required. In the LM model, the strain rate Reynolds number, which is a local variable, maps to the momentum thickness Reynolds number, which is nonlocal and plays an important role in transition prediction. The transported variables are the intermittency and the momentum thickness Reynolds number. The transport equation for the intermittency, γ, is given by,

$$\frac{\partial(\rho\gamma)}{\partial t} + \frac{\partial(\rho U_j\gamma)}{\partial x_j} = P_\gamma - E_\gamma + \frac{\partial}{\partial x_j}\left[(\mu + \frac{\mu_t}{\sigma_f})\frac{\partial\gamma}{\partial x_j}\right], \tag{2}$$

where ρ is the density, U is the velocity, P_γ is the intermittency source term, E_γ is the destruction/relaminarization source, μ is the molecular dynamic viscosity, μ_t is the eddy viscosity, and $\sigma_f = 1.0$. The intermittency is used to trigger the SST source terms. The second transport equation is written for the transition onset, which is triggered by the Reynolds number based on the momentum-thickness, $\tilde{R}e_{\theta_t}$, and can be written as,

$$\frac{\partial(\rho\tilde{R}e_{\theta_t})}{\partial t} + \frac{\partial(\rho U_j\tilde{R}e_{\theta_t})}{\partial x_j} = P_{\theta_t} + \frac{\partial}{\partial x_j}\left[\sigma_{\theta_t}(\mu + \mu_t)\frac{\partial\tilde{R}e_{\theta_t}}{\partial x_j}\right], \tag{3}$$

where P_{θ_t} is the source term and $\sigma_{\theta_t} = 2.0$. The latter constant controls the diffusion coefficient. The intermittency represents the probability of a fluid cell to be turbulent. Therefore, Eq. 2 allows the estimation of the extension of the transition region. Equation 3, for the momentum-thickness Reynolds transport equation, works as a sensor responsible for triggering the transition process, given that $\tilde{R}e_{\theta_t}$ indicates the point where it begins. To activate the turbulent kinetic energy production term, the LM model couples the intermittency function with the SST turbulent model. Such interaction occurs through the production term $\tilde{P}_k$,

$$\frac{\partial(\rho k)}{\partial t} + \frac{\partial(\rho u_j k)}{\partial x_j} = \tilde{P}_k - \tilde{D}_k + \frac{\partial}{\partial x_j}\left[(\mu + \sigma_k\mu_t)\frac{\partial k}{\partial x_j}\right], \tag{4}$$

$$\tilde{P}_k = \gamma_{eff}P_k, \tag{5}$$

where γ_{eff} is introduced in order to include separation effects in the formulation. Further information and the empirical correlations that complete the model can be found in the literature (Langtry and Menter, 2009). The Langtry-Menter transition model is able to correctly predict Tollmien-Schliting waves and bypass transition mechanisms.

The transition due to Tollmien-Schliting waves (Schubauer and Skramstad, 1948) usually takes place when the free-stream turbulence intensity is smaller than 1% (Mayle, 1991). The process reveals all phases of natural transition. On the other hand, bypass transition is characterized by freestream turbulence intensities larger than 1% and, although it is not fully understood, can be found in the presence of wall roughness (Langtry, 2006).

2.3 Spatial Discretization and Roe Scheme

The equations of the Langtry-Menter model have to be solved numerically. In order to do that, the finite-volume formulation (Hirsch, 1990) and the Roe Riemann solver (Roe, 1981) solver were used. The finite-volume formulation discretized in a control volume reads,

$$\frac{\partial(Q_i)}{\partial(t)} = \frac{1}{V_i}\sum_{k=1}^{n_f}[(E_(ek) - E_(vk)S_k)] \tag{6}$$

where *i* is the volume index, *k* is the face index, *nf* is the total number of faces in the control volume and S_k is the area normal vector.

The flux-difference splitting scheme of Roe is the most used approach on unstructured grids. It is an upwind flux-difference splitting (Roe, 1981) scheme and requires flow states to be specified on the left and the right side of the control volume face. In order to stabilize the solution, artificial dissipation has to be added. In the Roe scheme, the value of artificial dissipation is clipped with the eigenvalues of the Roe matrix and is entered by the user.

3. FLAT-PLATE TEST CASES

The first test performed here is for a zero-pressure gradient flat plate. The comparisons performed in the present work are based on the flat-plate experiments Savill (1993) and Schubauer and Klebanoff (1955), also on the data available from the investigations by Rumsey and Lee-Rausch (2015) and Coder (2018) for two different freestream turbulence intensities, Tu_i. The test cases analyzed consider one flow condition in which Tu_i is lower than 1% and another condition with Tu_i larger than this value. Therefore, the first test case will be referred to in the present paper as a transition due to Tollmien-Schliting wave instability test case (Case A), whereas the other corresponds to a flow with bypass transition (Case B). Both A and B cases share the same geometry with a 0 deg. angle of attack, based on the European Research Community on Flow Turbulence and Combustion (ERCOFTAC) T3A flat plate test case. The freestream speed is 69.438 m/s, the Mach number is 0.2, the reference length of the flat plate is 1m and the reference Reynolds number based on reference length is 5 million. The boundary conditions are imposed as farfield, adiabatic solid wall, symmetry, and in the inlet and outlet pressure is specified. Three different meshes are tested for the 3-D domain. The coarsest mesh has 26,578 cells, the intermediate one has 105,378 cells, and the finest mesh has 419,650 cells. All the three meshes can be found in the NASA Turbulence Modeling Resource website (https://turbmodels.larc.nasa.gov/).

For Case A, the first test performed includes the coarsest and the finest meshes with a freestream turbulence intensity of 0.3%. Figure 1 presents the skin friction coefficient (c_f), where it is possible to observe the transition locations for the numerical results together with the experimental data. The numerical results obtained here are for different values of artificial dissipation computed for the two meshes mentioned before, "c" stands for coarsest and "f" for finest. Herein, two values of dissipation, α, are tested, 0.005 and 0.001. Although there is a difference between the experimental data and the numerical results concerning the point of transition, it is possible to observe that the coarsest mesh displays more influence from the artificial dissipation than the finest one. In other words, for the the coarsest mesh there is a considerable improvement in the results when the lowest dissipation is used. However, for the finest mesh there is no significant change between the purple and green curves. On the interest of brevity, there are no results for Case B here, because it did not show sensitivity with respect to this parameter related to mesh refinement. In our numerical results, the TS wave-triggered transition fronts move downstream for increasingly higher artificial dissipation values. This is likely caused by excessive high dissipation values, which are preventing the modeled flow instabilities to grow. Therefore, lower values of artificial dissipation lead to better results.

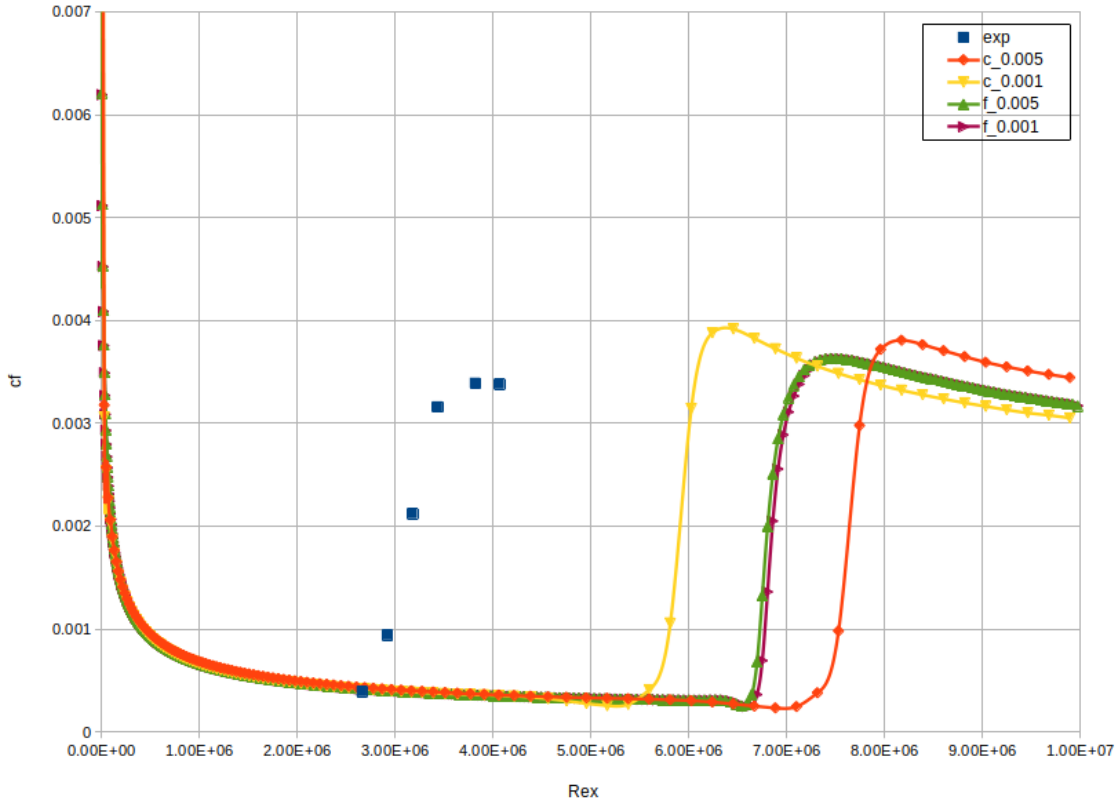

Figure 1: Effects of dissipation on the coarsest and finest mesh for the flat plate Case A.

Continuing with Case A, the second test includes the other parameter analyzed here, the eddy viscosity ratio, μ_t/μ, which is the other specification of the turbulence at the inlet boundary, together with the freestream turbulence intensity,

Tu_i. The eddy viscosity ratio can be related to the turbulent length scale, L, and it has an impact on transition. Both values can be related by

$$L = (\frac{\mu_t}{\mu})\frac{\mu}{\rho k^{\frac{1}{2}}}, \tag{7}$$

where ρ is the density and k is the turbulent kinetic energy. Figure 2 shows the results for the skin friction coefficient, where it is possible to observe the point of transition, considering the different values of eddy viscosity ratio studied: 1.0, 1.5, 2.0, 2.5. These results only consider an artificial dissipation of 0.001 for the two meshes, where "c" stands for coarse and "f" for finest. In this case, it can be observed that both meshes experience influence from the eddy viscosity ratio. There is a significant sensitivity in the studied parameters for the TS waves. Moreover, the turbulence length scale appears to be the parameter that is affecting the numerical results the most. This effect can be observed even more for the coarsest mesh. Numerical results for Case A indicate that the higher eddy viscosity ratio values lead to better results. However, the opposite trend is observed for Case B.

For Case B, numerical results for the skin friction coefficient (cf) are shown in Fig. 3 using the intermediate mesh for different values of eddy viscosity ratio. Numerical results are based on the T3A case compared with the experimental results by Coder (Coder, 2018). For this case, the values for the eddy viscosity ratio used are 11.9, 8.9, 5.9, and 2.9. By inspecting the plots in Fig. 3, one can see that lower values for the eddy viscosity ratio lead to better results for the transition location.

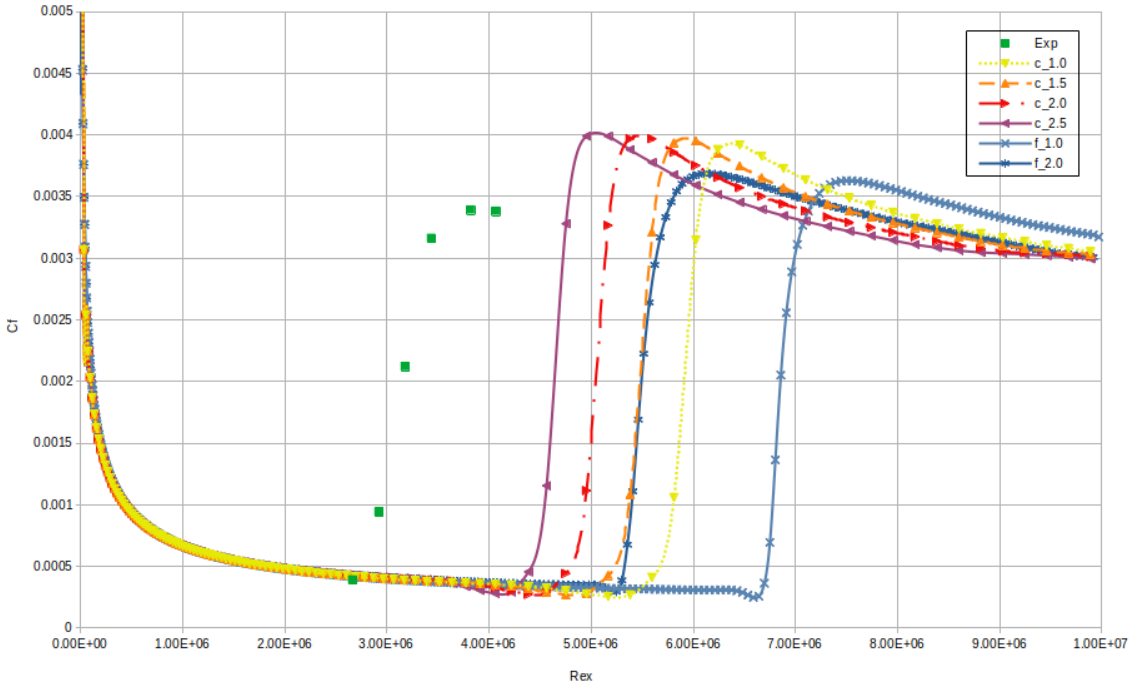

Figure 2: Effects of the eddy viscosity ratio on the coarsest and finest mesh for the flat plate Case A.

4. NLF(1)-0416 TEST CASE

Our next test case considers the NLF(1)-0416 airfoil. The NLF(1)-0416 airfoil was designed by Somers and tested in the NASA Langley Low-Turbulence Pressure Tunnel (LTPT) (Somers, 1981). Since there are no experimental results for bypass transition, only transition caused by the amplification of Tollmien-Schliting waves is tested. The test case represented here considers a 0 deg. angle of attack with a fine mesh containing 372,000 cells, which was created by the authors based on the guidelines proposed by Coder (2018). We use farfield and viscous wall boundary conditions. The freestream parameters are a Mach number of 0.2, a Reynolds number of 4 million based on the airfoil chord of 1m, and the freestream speed is 69.438 m/s. We use a freestream turbulent intensity of 0.15%, and consider freestream eddy viscosity ratios of 1 and 10. All numerical results are compared to experimental data from Somers (1981) and numerical simulations from Halila *et al.* (2019b). Skin friction results are shown in Fig. 4. There are no significant differences in the results for the NLF(1)-0416 airfoil for the different values of artificial dissipation using a fine mesh of good quality. The numerical results here obtained for the eddy viscosity ratio have a good agreement with expected results compared to (Halila *et al.*, 2019b).

Figure 5 represents the pressure coefficient results, and these results are in agreement with the expected results compared to (Halila *et al.*, 2019b). The pressure coefficient is only affected by the freestream eddy viscosity values in a region

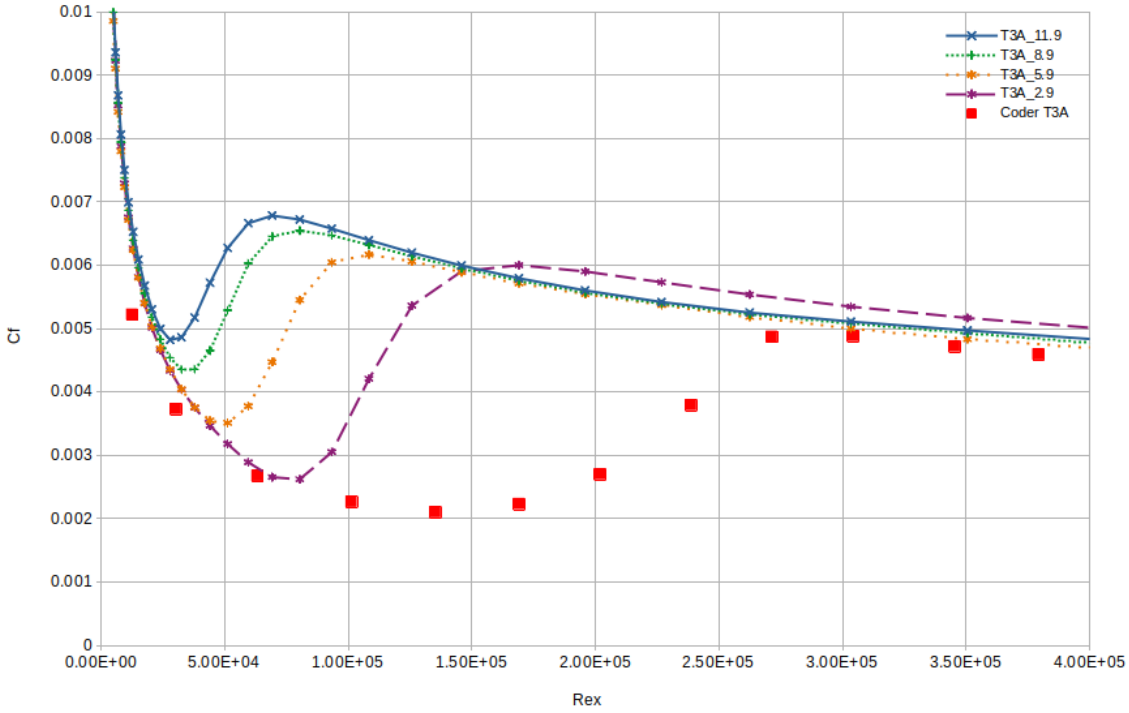

Figure 3: Effects of the eddy viscosity ratio on the intermediate mesh for the flat plate Case B.

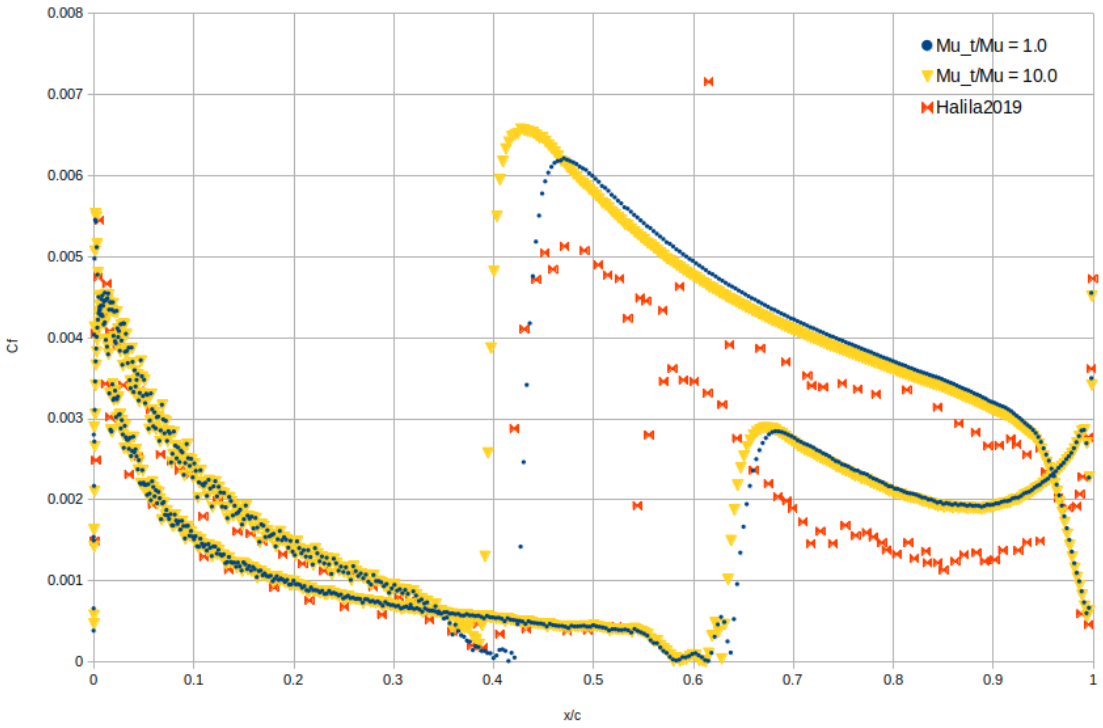

Figure 4: Effects of the eddy viscosity ratio for the NLF(1)-0416 airfoil.

around the transition front. Table 1 lists numerical and experimental (Somers, 1981) transition locations for this test case.

Table 1: Numerical and experimental transition locations (x/c_{tr}) for the NLF(1)-0416 airfoil.

Side	**Results**	**Experiment**
Upper	0.42	0.38
Lower	0.63	0.52

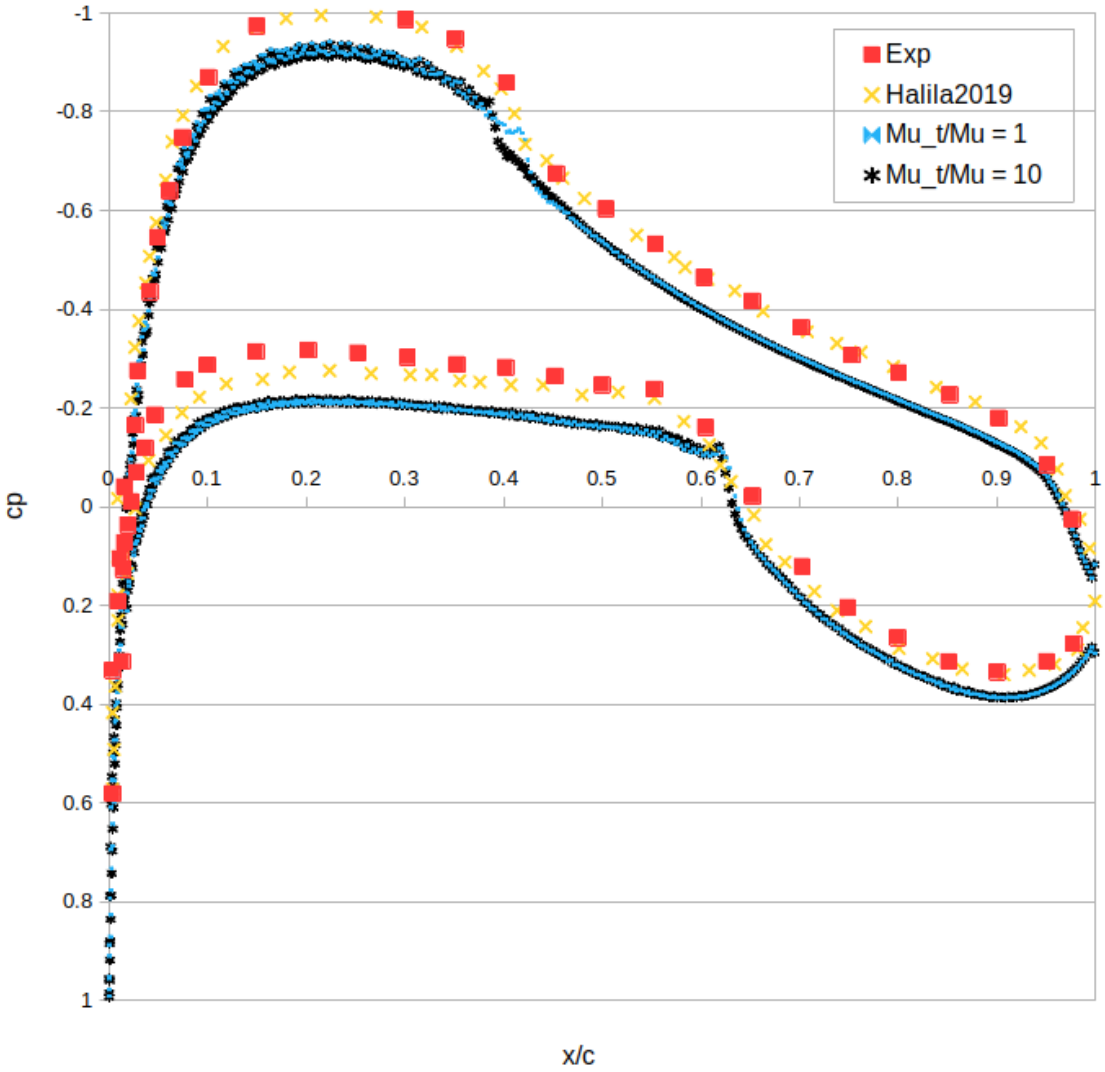

Figure 5: Pressure coefficient for both cases of eddy viscosity ratio for the NLF(1)-0416 airfoil.

5. CONCLUDING REMARKS

Transition to turbulence plays relevant roles in many engineering applications. In the aerospace industry, transition prediction is relevant for the design of high-performance wings, high-lift devices, horizontal and vertical tails, and nacelles. Transition to turbulence can be accounted for, in daily applications, by using flow stability analysis. Flow stability analysis is able to track the hydrodynamic modes evolution in space and time, but is not fully-compatible with modern parallel computing techniques. To address this shortcoming, modified Reynolds-Averaged Navier-Stokes (RANS) models that use additional transport equations to reproduce the transition to turbulence effects in complex computational fluid dynamics (CFD) simulations were proposed.

In this work, we perform numerical investigations considering transitional flows as predicted by the Langtry-Menter (LM) transition model. Relevant parameters such as mesh refinement, artificial dissipation, and eddy viscosity ratio are used to investigate variations on the predicted transition front. We consider two test cases, namely a flat plate geometry and the NLF(1)-0416 single-element airfoil.

We observed some mismatches between predicted and experimental transition fronts for the flat plate test cases. This lead us to believe that there is a certain sensitivity in the numerical code for this specific geometry. Even though the flat plate represents a simple geometry, the sudden change toward a viscous wall boundary condition in the leading edge region is a challenge for the numerical solution. Therefore, we believe that the reported issues with the flat plate results are partially caused by the geometry leading edge. The effects caused by the geometry leading edge are likely combined with the code sensitivity observed for this test case, the mix of these factors leading to the issues reported here.

The Langtry-Menter transition model is based on distinct empirical correlations for each of the different transition mechanisms. Our flat plate numerical simulations lead to the observation that, for the Tollmien-Schliting wave results,

there is a more pronounced sensitivity to mesh refinement, artificial dissipation, and eddy viscosity ratio than for the cases where bypass transition takes place. This indicates that the distinct empirical correlations that are part of the model are excited by the factors above in different ways. The NLF(1)-0416 airfoil numerical results did not reveal sensitivity to artificial dissipation for a fine mesh, but some sensitivity due to the eddy viscosity ratio was observed. The results for the NLF(1)-0416 airfoil are in engineering agreement with experimental and numerical data from the literature.

Finally, for all test cases, the most important aspect to be aware of is the dependence of the transition location on the inflow variables. Current investigations are addressing the optimal values for each of the parameters mentioned in this paper for a variety of test cases and flight conditions.

6. ACKNOWLEDGEMENTS

The authors gratefully acknowledge the support provided by Fundação de Amparo à Pesquisa do Estado de São Paulo, FAPESP, through a doctoral scholarship for the first author under Grant No. 2021/00031-0. The authors also gratefully acknowledge the support for the present research provided by Conselho Nacional de Desenvolvimento Científico e Tecnológico, CNPq, under the Research Grant No. 309985/2013-7. The work is also supported by computational resources of the Center for Mathematical Sciences Applied to Industry (CeMEAI), funded by FAPESP under the Research Grant No. 2013/07375-0. Additional support to the fourth author under the FAPESP Research Grant No. 2013/07375-0 is also acknowledged.

7. REFERENCES

Bigarella, E.D.V., 2007. *Advanced Turbulence Modelling for Complex Aerospace Applications*. Ph.D. thesis, Instituto Tecnológico de Aeronáutica, São José dos Campos, Brasil.

Bigarella, E.D.V. and Azevedo, J.L.F., 2007. "Advanced eddy-viscosity and Reynolds-stress turbulence model simulations of aerospace applications". *AIAA Journal*, Vol. 45, No. 10, pp. 2369–2390.

Carvalho, L.M., Silva, R.G. and Azevedo, J.L., 2018. "Numerical study of transitional flows over aerospace configurations". In *Proceedings of the 2018 Applied Aerodynamics Conference, Aviation Forum,* AIAA Paper No. 2018-4209. doi:10.2514/6.2018-4209.

Chien, K.Y., 1982. "Predictions of channel and boundary-layer flows with a low-Reynolds-number turbulence model". *AIAA Journal*, Vol. 20, pp. 33–38.

Coder, J.G., 2018. "Standard test cases for transition model verification and validation in computational fluid dynamics". In *Proceedings of the 2018 AIAA Aerospace Sciences Meeting, AIAA SciTech Forum,* AIAA Paper No. 2018-0029. Kissimmee, FL. doi:10.2514/6.2018-0029.

Ghasemi, E., McEligot, D., Nolan, K., Crepeau, Siahpush, A., Budwig, R. and Tokuhiro, A., 2014. "Effects of adverse and favorable pressure gradients on entropy generation in a transitional boundary layer region under the influence of freestream turbulence". *International Journal of Heat and Mass Transfer*, Vol. 77, pp. 475–488.

Halila, G.L.O., Antunes, A.P., Silva, R.G. and Azevedo, J.L.F., 2019a. "Effects of boundary layer transition on the aerodynamic analysis of high-lift systems". *Aerospace Science and Technology*, Vol. 90, pp. 233–245. doi: 10.1016/j.ast.2019.04.051.

Halila, G.L.O., Bigarella, E.D.V., Antunes, A.P. and Azevedo, J.L.F., 2018. "An efficient setup for freestream turbulence on transition prediction over aerospace configurations". *Aerospace Science and Technology*, Vol. 81, pp. 259–271. doi:10.1016/j.ast.2018.08.013.

Halila, G.L.O., Bigarella, E.D.V. and Azevedo, J.L.F., 2016. "A numerical study on transitional flows using a correlation-based transition model". *Journal of Aircraft*, Vol. 53, No. 4, pp. 922–941. doi:10.2514/1.C033311.

Halila, G.L.O., Chen, G., Shi, Y., Fidkowski, K.J., Martins, J.R.R.A. and Mendonça, M., 2019b. "High-Reynolds number transitional flow prediction using a coupled discontinuous-Galerkin RANS PSE framework". *Aerospace Science and Technology*, Vol. 91, pp. 321–336. doi:10.1016/j.ast.2019.05.018.

Halila, G.L.O., Fidkowski, K.J. and Martins, J.R.R.A., 2021. "Toward automatic parabolized stability equation-based transition-to-turbulence prediction for aerodynamic flows". *AIAA Journal*, Vol. 59, No. 2, pp. 462–473. doi: 10.2514/1.J059516.

Halila, G.L.O., Martins, J.R.R.A. and Fidkowski, K.J., 2020. "Adjoint-based aerodynamic shape optimization including transition to turbulence effects". *Aerospace Science and Technology*, Vol. 107, p. 106243. doi: 10.1016/j.ast.2020.106243.

Hirsch, C., 1990. *Numerical Computation of Internal and External Flows*. Wiley.

Klebanoff, P.S., Tidstrom, K.D. and Sargent, L.M., 1962. "The three-dimensional nature of boundary layer instability". *Journal of Fluid Mechanics*, Vol. 12, pp. 1–24.

Langtry, R.B., 2006. *A Correlation-Based Transition Modeling using Local Variables for Unstructured Parallelized CFD Codes*. Ph.D. thesis, Universität Stuttgart, Stuttgart, Germany.

Langtry, R.B. and Menter, F.R., 2009. "Correlation-based transition modeling for unstructured parallelized computational

dynamics codes". *AIAA Journal*, Vol. 47, No. 12, pp. 2894–2906.

Mayle, R.E., 1991. "The role of laminar-turbulent transition in gas turbine engines". *ASME Journal of Turbomachinery*, Vol. 113, pp. 509–537.

Menter, F.R., 1994. "Two-equation eddy viscosity turbulence models for engineering applications". *AIAA Journal*, Vol. 32, No. 8, pp. 1598–1605.

Roe, P.L., 1981. "Approximate riemann solvers, parameter vectors, and difference schemes". *Journal of Computational Physics*, Vol. 43, pp. 357–372.

Rumsey, C.L. and Lee-Rausch, E.M., 2015. "NASA trapezoidal wing computations including transition and advanced turbulence modeling". *Journal of Aircraft*, Vol. 52, pp. 496–509.

Saric, W.S. and Dagenhart, J.R., 1999. "Crossflow stability and transition experiments in swept-wing flow". NASA TP-1999-209344, NASA.

Savill, A.M., 1993. "Some recent progress in the turbulence modeling of by-pass transition". In *Near-Wall Turbulent Flows, edited by R. M. C. So and C. G. Speziale and B. E. Launder,* Elsevier.

Schubauer, G.B. and Klebanoff, P.S., 1955. "Contributions on the mechanics of boundary layer transition". Technical Report NACA TN 3489.

Schubauer, G.B. and Skramstad, H.K., 1948. "Laminar boundary layer oscillations and transition on a flat plate". Technical Report NACA Report 909, NACA.

Shi, Y., Mader, C.A., He, S., Halila, G.L.O. and Martins, J.R.R.A., 2020. "Natural laminar flow airfoil design using a discrete adjoint approach with RANS-e^n transition prediction". *AIAA Journal*, Vol. 58, No. 11. doi:10.2514/1.J058944.

Smith, A.M.O. and Gamberoni, N., 1956. "Transition, pressure gradient and stability theory". Douglas Aircraft Company Report ES 26388, Douglas Aircraft Company, Long Beach, CA.

Somers, D.M., 1981. "Design and experimental results for a natural-laminar-flow airfoil for general aviation applications". Technical Report NASA TP-1681, National Aeronautics and Space Administration – NASA.

Spalart, P.R. and Allmaras, S.R., 1994. "A one-equation turbulence model for aerodynamic flows". *Recherche Aerospatiale*, Vol. 1, pp. 5–21.

Versteeg, K.H. and Malalasekera, W., 2007. *An Introduction to Computational Fluid Dynamics*. Pearson Education Limited, 2nd edition.

Wilcox, D.C., 1994. *Turbulence Modeling for CFD*. DCW Industries, Incorporated.

Wilcox, D.C., 2008. "Formulation of the k-omega turbulence model revisited". *AIAA Journal*, Vol. 46, pp. 2823–2838.

8. RESPONSIBILITY NOTICE

The authors are solely responsible for the printed material included in this paper.